

Original article

Unsteady-state CO₂ foam injection for increasing enhanced oil recovery and carbon storage potential

Aleksandra Sæle^{✉*}, Arne Graue, Zachary Paul Alcorn

Department of Physics and Technology, University of Bergen, Bergen, Norway

Keywords:

CO₂ foam
unsteady-state injection
mobility control
carbon storage potential

Cited as:

Sæle, A., Graue, A., Alcorn, Z. P. Unsteady-state CO₂ foam injection for increasing enhanced oil recovery and carbon storage potential. *Advances in Geo-Energy Research*, 2022, 6(6): 472-481.

<https://doi.org/10.46690/ager.2022.06.04>

Abstract:

The efficiency of CO₂ injection for enhanced oil recovery and carbon storage is limited by severe viscosity and density differences between CO₂ and reservoir fluids and reservoir heterogeneity. In-situ generation of CO₂ foam can improve the mobility ratio to increase oil displacement and CO₂ storage capacity in geological formations. The aim of this work was to investigate the ability of CO₂ foam to increase oil production and associated CO₂ storage potential, compared to other CO₂ injection methods, in experiments that deploy field-scale injection strategies. Additionally, the effect of oil on CO₂ foam generation and stability was investigated. Three different injection strategies were implemented in the CO₂ enhanced oil recovery and associated CO₂ storage experiments: pure CO₂ injection, water-alternating-gas and surfactant-alternating-gas. Foam generation during surfactant-alternating-gas experiments showed reduced CO₂ mobility compared to water-alternating-gas and pure CO₂ injections indicated by the increase in apparent viscosity. CO₂ foam increased oil recovery by 50% compared to pure CO₂ injection and 25% compared to water-alternating-gas. In addition, CO₂ storage capacity increased from 12% during pure CO₂ injection up to 70% during surfactant-alternating-gas injections. Experiments performed at high oil saturations revealed a delay in foam generation until a critical oil saturation of 30% was reached. Oil/water emulsions in addition to CO₂ foam generation contributed to CO₂ mobility reduction resulting in increased CO₂ storage capacity with foam.

1. Introduction

Carbon capture, utilization, and storage (CCUS) is an important contributor to the ongoing transition to a net-zero carbon emission society. In the context of this work, CCUS involves capturing anthropogenic CO₂ from point sources and injecting it into geological formations for energy production and permanent storage (IPCC, 2005). Injection of CO₂ for enhanced oil recovery (EOR) has been performed for over 50 years with commercial success. CO₂ is an excellent solvent for EOR because, at typical reservoir conditions, it is miscible with most of crude oils and may swell the oil, reduce its viscosity and the interfacial tension between oil and water, which all contribute to increased oil recovery (Lee and Kam, 2013). Although utilization of CO₂ for EOR has several benefits there are disadvantages associated with the

density and viscosity differences between the injected CO₂ and reservoir fluids. Common challenges are gravity override, viscous fingering and early gas breakthrough which result in reduced oil recovery and lower carbon storage capacity (Lake et al., 2014). These challenges can be mitigated by reducing CO₂ mobility (Hanssen et al., 1994; Enick et al., 2012).

Common CO₂ mobility control methods include water-alternating-gas (WAG), foams and polymers (Enick et al., 2012). WAG is a method where water and a gas are injected into the porous media in alternating slugs. During WAG injection, the water slugs reduce the relative permeability of the gas to increase volumetric sweep efficiency. WAG will therefore provide CO₂ mobility control by reducing the effect of viscous fingering and early gas breakthrough (Christensen et al., 2001; Massarweh and Abushaikha, 2021). Gravity override can still be a challenge because of density and viscosity diffe-

Table 1. Core properties.

Properties	SS1	SS2
Length (cm)	16.05 ± 0.01	15.55 ± 0.01
Diameter (cm)	3.87 ± 0.01	3.89 ± 0.01
Pore Volume (ml)	41.99 ± 0.01	41.14 ± 0.01
Porosity (%)	22.24 ± 0.05	22.29 ± 0.05
Permeability (D)	2.26 ± 0.03	2.47 ± 0.02
Experiments	Foam quality rate scans	EOR

rences between the injected gas and fluids in the reservoir. The injected CO₂ can be foamed to increase the viscosity of CO₂ and prevent flow instabilities (Rossen, 1996; Skauge et al., 2002; Talebian et al., 2014).

Foam is a colloidal dispersion where gas is dispersed in continuous liquid films called lamellae (Falls et al., 1989; Tadros, 2017). Lamellae are thermodynamically unstable but can be stabilized by a foaming agent, most commonly a surfactant (Schramm, 1994). Foam increases the viscosity of CO₂, thereby reducing CO₂ mobility and improving displacement (Talebian et al., 2014). The efficiency of CO₂ foam for combined EOR and CO₂ storage strongly depends on foam strength and stability, which is influenced by the presence of oil. Several studies report that oil can hinder foam generation and can destabilize foam by spontaneously spreading on the liquid films, resulting in an unstable oil film and bubble coalescence (Ross and McBain, 1944). Others report generation of oil/water emulsions in addition to foam, which increases the capillary number and is beneficial for oil recovery (Amirmoshiri et al., 2018; Alcorn et al., 2020). The effect of oil on foam is an area under active investigation.

CO₂ foam is generated in-situ by injecting CO₂ and a foaming solution, either simultaneously (co-injection) or by injecting alternating slugs of foaming solution and CO₂ surfactant-alternating-gas (SAG) (Farajzadeh et al., 2012). At laboratory scale, co-injection is the most common injection strategy because of the ability to achieve steady-state for deriving foam model parameters. Co-injection can be difficult to implement at field-scale because of operational limitations (Hoefner and Evans, 1995). Extremely low injectivities, rapid pressure increases, and challenges associated with downhole corrosion are some of challenges that has led to most field tests using SAG as the injection strategy (Chou et al., 1992; Hoefner and Evans, 1995; Shan and Rossen, 2004).

Few attempts have been made to characterize unsteady-state in-situ CO₂ foam behavior during injection of alternating slugs. Therefore, this study aims to establish a knowledge base and procedure for investigating core-scale CO₂ foam injection strategies for EOR and CO₂ storage. The primary objective was to reduce CO₂ mobility, through the generation of foam, in experiments that are representative of field-scale injection strategies. Three different CO₂ injection strategies were implemented and compared based upon their impact on oil recovery and CO₂ storage. A secondary objective was to investigate the effect of oil on CO₂ foam generation and

stability.

2. Materials and experimental set-up

2.1 Core material

The experiments were performed on two outcrop Bentheimer core plugs with similar properties (Table 1). Bentheimer is a water-wet, homogenous sandstone consisting mainly of quartz, feldspar and clay (Peksa et al., 2015). Sandstone reservoirs are the most common reservoir type in the world and are good candidates for CO₂ storage (Bjørlykke, 2010). Before the experiments the core plugs were cut to the desired length, cleaned, and dried at 60 °C for 72 hours. Then the core plugs were fully saturated with brine under vacuum. The porosity and pore volume of the core plugs were calculated based on weight difference between a dry and a fully saturated core. Absolute brine permeability was measured using Darcy's law for three different injection rates. The core properties are shown in Table 1.

2.2 Fluids

Table 2 shows the fluid properties. Brine consisting of 3.5 wt% NaCl was used for saturation of the core plugs and for waterfloods. To generate CO₂ foam, a nonionic water-soluble surfactant (Surfonic L24-22, Huntsman, TX, USA) was used as the foaming agent. This surfactant was previously tested at core- and field-scale and has shown promising effect on CO₂ mobility reduction (Alcorn et al., 2020a, 2020b). The surfactant was dissolved in brine to make foaming solutions with desired concentrations (Table 2). Both concentrations were above the critical micelle concentration of the surfactant (Sharma, 2019). EOR experiments were performed at first-contact miscible conditions using a mineral oil, n-Decane as the oleic phase. The core plugs were cleaned between each experiment using 2-propanol-water-azeotrope (IPA).

2.3 Experimental set-up

The core plug was wrapped in a nickel foil to reduce radial CO₂ diffusion into the surrounding Viton rubber sleeve. The core was mounted in a vertically positioned biaxial Hassler core holder and placed in a heating cabinet. The experimental conditions were 40 °C and 180 bar with an overburden pressure of 240 bar. At these conditions CO₂ is supercritical and miscible with n-Decane. The pressure in the system was maintained by two Equilibar back pressure regulators connected in series to reduce pressure fluctuations. The confinement pressure was controlled using an ISCO pump and the fluids were injected using three different Quizix pumps (Fig. 1). A differential pressure transducer and two absolute pressure transducers were used to measure and control the pressure response. The produced fluids were depressurized and collected at atmospheric conditions. The liquids were collected in a glass cylinder and CO₂ was vented out through an adsorption column. Volume and mass of the produced liquids were measured, and material balance was used to calculate fluid saturation in the core and to estimate the amount CO₂ stored in the core.

Table 2. Fluid properties.

Fluids	Composition
Brine	3.5 wt% NaCl
Foaming solutions	0.25 wt% Surfonic L24-22, Brine 0.50 wt% Surfonic L24-22, Brine
Oil	n-Decane, C ₁₀ H ₂₂
CO ₂	> 99.99% CO ₂
IPA	87.7 wt% 2-propanol

3. Methods

3.1 Foam quality and rate scans

Foam strength and stability is impacted by foam quality and injection rate (Chang and Grigg, 1999). Steady state co-injections of CO₂ and foaming solution were performed as gravity stable assisted injection from top to determine the optimal gas fraction and injection rate that will generate foam with the highest apparent viscosity. Foam quality scans were performed with a drainage-like co-injection with increasing gas fraction (fg). The superficial velocity was constant during foam quality scans (2 and 4 ft/day) and the gas fraction monotonically increased from 0.3 to 1.0. The core plug was saturated with brine before the injections started. Each gas fraction was held constant until steady state was obtained. Apparent viscosity was calculated at steady state for each gas fraction. The gas fraction at which apparent viscosity was highest was used for rate scans. Foam apparent viscosity (μ_{app}) was calculated based on the differential pressure and is defined as:

$$\mu_{app} = \frac{k}{\mu_g + \mu_l} \nabla \rho \quad (1)$$

where k is the absolute permeability of the core, μ_g and μ_l are respectively gas and liquid superficial velocities, and $\nabla \rho$ is the pressure gradient across the core (Jones et al., 2016). A higher apparent viscosity corresponds to stronger foam.

Rate scans were also performed to determine the influence of injection rate on foam strength and stability. During rate scans, CO₂ and foaming solution were co-injected at constant foam quality, as determined from the quality scan, with increasing superficial velocity from 2 to 12 ft/day. Each rate was held constant until steady state was obtained. An optimal velocity was chosen based on the apparent viscosity results.

3.2 Injection strategies

Three different injection strategies were implemented in the CO₂ EOR and associated CO₂ storage experiments: pure CO₂ injection, WAG and SAG. For all experiments the core plug was 100% saturated with brine before primary drainage with oil until a water saturation between 0.30 and 0.40 was reached. After drainage, the core plug was flooded with water or foaming solution to obtain a residual oil saturation of approximately 0.30. For some experiments the core was not waterflooded and WAG and SAG was implemented directly

after drainage. Fig. 2 shows the injection schemes used during EOR experiments. Each experiment was performed at least twice and the procedures are described below.

(i) Pure CO₂ Injection

During pure CO₂ injection, supercritical CO₂ was injected into the core at a superficial velocity of 4 ft/day. The injection lasted for a total of 8 to 10 pore volumes injected. Two types of experiments were performed: CO₂ injection after waterflood and CO₂ injection after injection of foaming solution (Fig. 2). Differential pressure and fluid production were measured during the experiments.

(ii) WAG and SAG

During WAG and SAG, 18 cycles (approximately 3.5 Pore Volume (PV) injected) of brine or foaming solution and CO₂ were injected (Fig. 2). Each cycle consisted of one brine or foaming solution slug and one CO₂ slug. The volumetric ratio between the slugs was 0.60 to achieve the desired gas fraction as determined from the foam quality scans. After completing the WAG and SAG cycles, pure CO₂ was injected for additional 5 to 6 pore volumes to study the dry out effect, a phenomenon where foam collapses as a result of low foaming solution saturation and high gas fraction. Superficial velocity during WAG and SAG injections was 4 ft/day. Two different foaming solution concentrations were tested during SAGs. The experiments were conducted after waterflood (Fig. 2(a)) and after drainage (Fig. 2(b)).

3.3 CO₂ storage capacity estimation

The CO₂ storage capacity was defined as the fraction of pore volume available for storing CO₂. During the experiments, the volume and mass of produced liquids was precisely measured and the CO₂ storage potential was calculated using the equation below:

$$\text{CO}_2 \text{ storage potential (\%)} = \frac{V_{o,p} + V_{w,p} - V_{w,i}}{V_p} \times 100\% \quad (2)$$

where $V_{o,p}$, $V_{w,p}$, $V_{w,i}$ are respectively volume of oil produced, volume of water, and volume of water injected; V_p is pore volume of the core plug. The volume of CO₂ dissolved in water- and oil-phase was not included in the estimations.

4. Results and discussion

4.1 Foam quality and rate scans

Fig. 3 shows apparent viscosity as a function of gas fraction during co-injections at 2 ft/day (a) and 4 ft/day (b). Two different velocities were tested to investigate the effect of superficial velocity on foam strength. Foam was generated at the lowest gas fraction (0.30) indicated by high apparent viscosity compared to no foam experiment (Fig. 3(a), black dots). Foam apparent viscosity increased until a peak at gas fraction between 0.50 and 0.60. Beyond this point, foam strength decreased as the gas fraction increased because foam texture became coarser when a limiting capillary pressure was reached (Khatib et al., 1988; Farajzadeh et al., 2015). Previous researchers have observed an increase in the optimal gas fraction with increasing velocity (Osterloh and Jante, 1992; Alvarez et al., 2001). However, this behavior was not observed

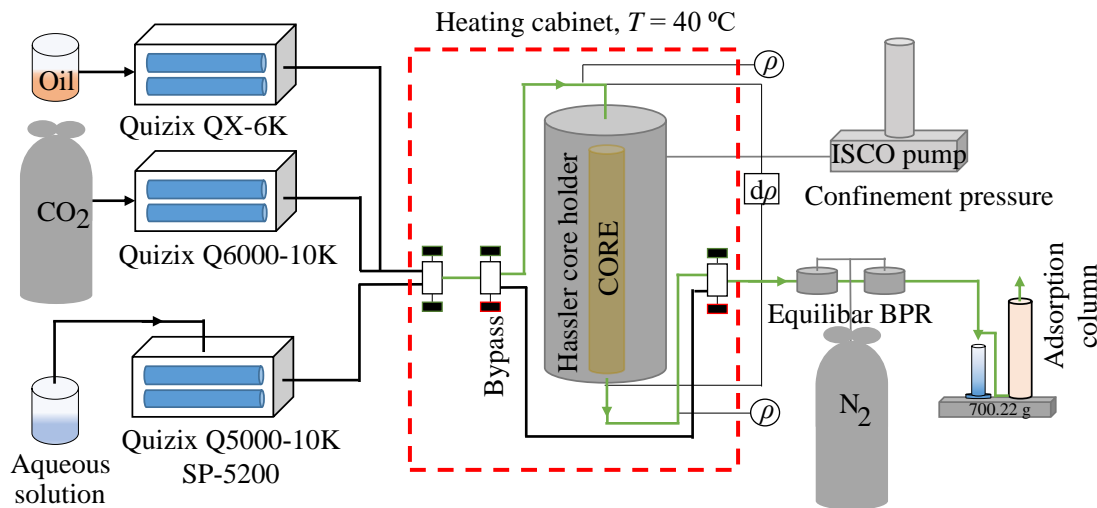


Fig. 1. Experimental set-up. Brine saturated core plug was mounted inside a core holder in a heating cabinet. Green lines represent fluid flow during the experiment. Two back pressure regulators connected in series maintained desired system pressure. A differential pressure transducer and two absolute pressure transducers were used to control and measure the pressure response. The produced fluids were depressurized, collected and measured at atmospheric conditions.

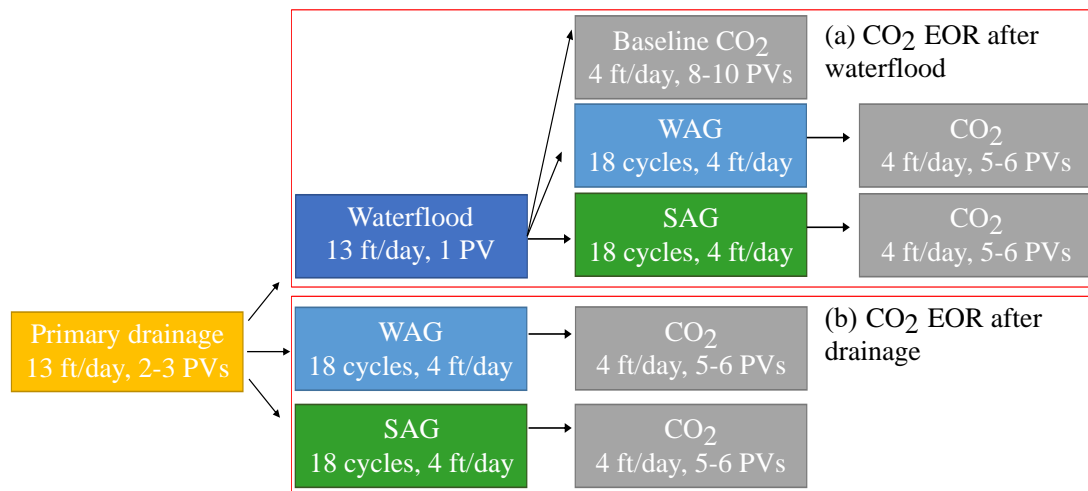


Fig. 2. Injection schemes. Each experiment started with primary drainage, then different CO₂ injection strategies were implemented either after waterflood (a) or directly after drainage (b). Three injection strategies were performed: pure CO₂ injection, WAG and SAG.

here and the optimal gas fraction was between 0.50 and 0.60 for both superficial velocities.

The effect of a lower surfactant concentration on foam strength was observed at lower superficial velocity (Fig. 3(a)). Foam apparent viscosity was slightly higher using 0.50 wt% foaming solution compared to 0.25 wt%. Alcorn et al. (2019) reported the same behavior using foaming solutions of 1 wt% and 0.50 wt% with the same surfactant. Their results showed that reduction of surfactant concentration did not reduce the efficiency on EOR and CO₂ storage which is beneficial for field-scale applications. At higher superficial velocity the apparent viscosity was not affected by surfactant concentration (Fig. 3(b)). Comparison of the two injection velocities showed slightly stronger foam generation at higher velocity. Based on the foam quality scans, 0.60 was identified

as the optimal gas fraction for the rate scans.

Fig. 4 shows apparent viscosity as a function of superficial velocity using foaming solutions with 0.25 wt% (green) and 0.50 wt% (red) surfactant concentration. Results showed a near-Newtonian foam behavior where foam apparent viscosity was similar and independent of superficial velocity. For 0.25 wt% foaming solution, the average apparent viscosity was 26.8 ± 4.7 cP and for 0.50 wt% foaming solution the average apparent viscosity was 26.6 ± 1.4 cP. The average values are within the uncertainty range of each measurement. Many studies report shear-thinning behavior where apparent viscosity increases with decreasing superficial velocity for surfactant-stabilized foams (Lee and Heller, 1990; Rognmo et al., 2017). However, this behavior was not observed during the experiments. Alvarez et al. (2001) have reported similar

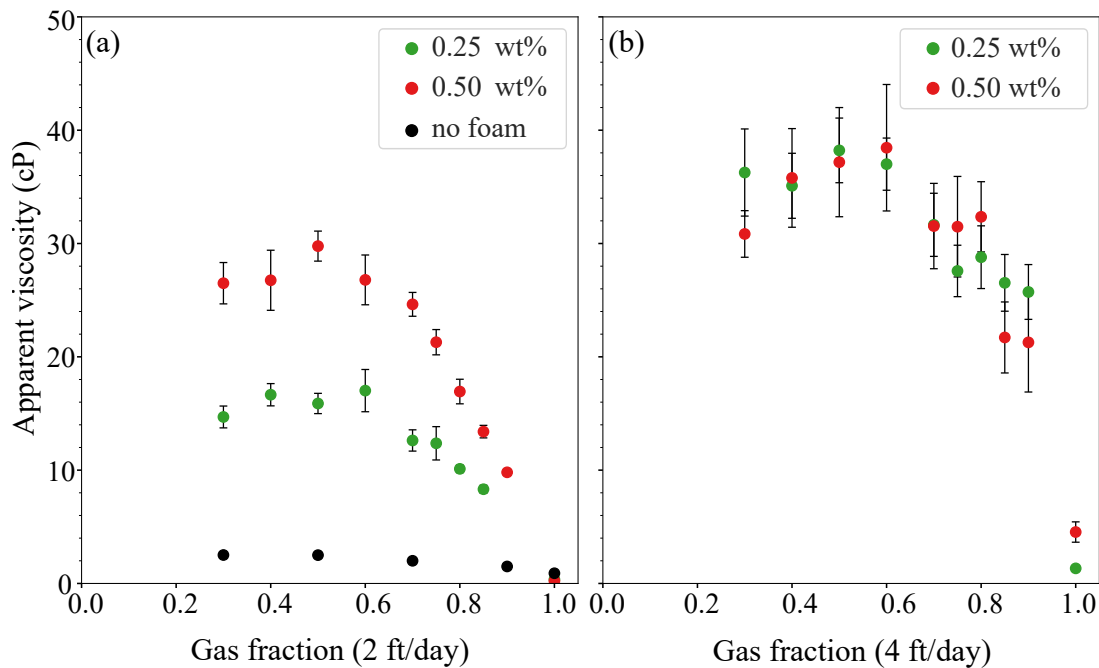


Fig. 3. Apparent viscosity as a function of gas fraction during steady state co-injection using two surfactant concentrations. Left graph is at superficial velocity of 2 ft/day and right at 4 ft/day. Each point was calculated when steady state was obtained. Injection without foaming solution (black dots, no foam) has been performed for comparison. Stronger foam generation was observed using higher surfactant concentration. Highest apparent viscosity was at gas fraction between 0.50 and 0.60.

behavior using a nonionic surfactant. The behavior is not fully understood but may be explained by pore geometry. It has been reported that pore throat size and pore angularity have an effect on foam generation and stability due to the effect on capillary pressure (Osei-Bonsu et al., 2018). Based on the results from rate scans, 4 ft/day was chosen as superficial velocity for the following EOR experiments.

4.2 Injection strategies for CO₂ and carbon storage

4.2.1 Pure CO₂ injection after waterflood

A baseline CO₂ injection was performed where supercritical CO₂ was injected into the core after waterflood to investigate CO₂ EOR and associated CO₂ storage. Fig. 5 shows apparent viscosity and recovery factors for baseline CO₂ injection (gray). Results showed low apparent viscosity because no foam was generated in absence of surfactant. The results also showed that 45% of original oil in place (OOIP) was recovered during waterflood and only 8% of OOIP was recovered during the subsequent CO₂ injection. CO₂ is miscible with n-Decane therefore high oil recovery was expected (Song et al., 2011). Low recovery can be explained by water shielding, a phenomenon where oil droplets are trapped within the water phase and are not in contact with the solvent. Earlier studies have shown that water shielding is significant especially for water-wet cores (Shelton and Schneider, 1975; Muller and Lake, 1991). Poor sweep efficiency due to rock heterogeneity can also reduce oil recovery (Chang et al., 1990). Pini et al. (2013) have shown that there is a degree

of heterogeneity in apparently homogenous sandstone cores which will affect the displacement front. Water recovery factor during the CO₂ injection was low (11%) as shown in Fig. 5. Poor water displacement can be explained by the high CO₂ mobility compared to water which lead to viscous fingering and early gas breakthrough (Lake et al., 2014).

4.2.2 Pure CO₂ injection after foaming solution injection

The effect of foam on CO₂ EOR efficiency and CO₂ storage capacity was evaluated by injecting foaming solution, rather than only waterflooding, prior to CO₂ injection. Fig. 5 shows the apparent viscosity and recovery factors as a function of PVs injected for baseline CO₂ injection after waterflood (gray) and CO₂ injection after foaming solution injection (green). Foam was generated as soon as CO₂ injection started into the core as indicated from the rapid increase in apparent viscosity (Fig. 5, green solid curve). The apparent viscosity increased until a peak of approximately 9 cP was reached, before decreasing and indication of foam coalescence. The reduction in water saturation and development of continuous CO₂ flow paths not impeded by lamella caused the foam to dry out (Farajzadeh et al., 2015; Benali et al., 2022). After several PVs injected, the apparent viscosity remained slightly higher than for the baseline experiment indicating decreased CO₂ mobility due to foam generation. The calculated recovery factors showed a positive effect of foam on both oil and water displacement. The total oil recovery was 53% for the experiment without foam and was 78% for the experiment with foam. Water recovery was also significantly higher for the experiment with foam where 60% of the water was displaced

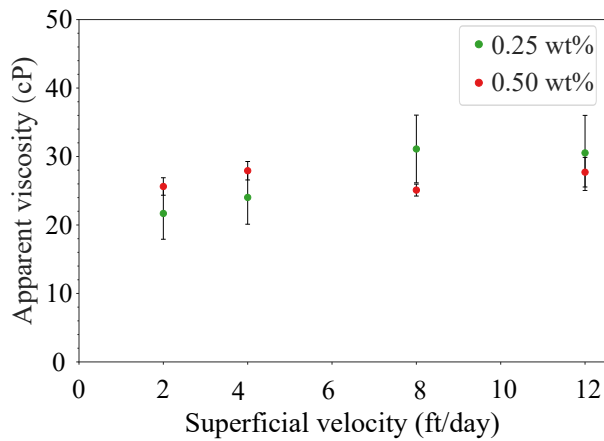


Fig. 4. Apparent viscosity as a function of superficial velocity for steady state co-injection of CO₂ and foaming solutions with 0.25 wt% (green) and 0.50 wt% (red) surfactant concentrations. Gas fraction was 0.60 for both. Near-Newtonian behavior was observed as foam apparent viscosity was independent of the velocity.

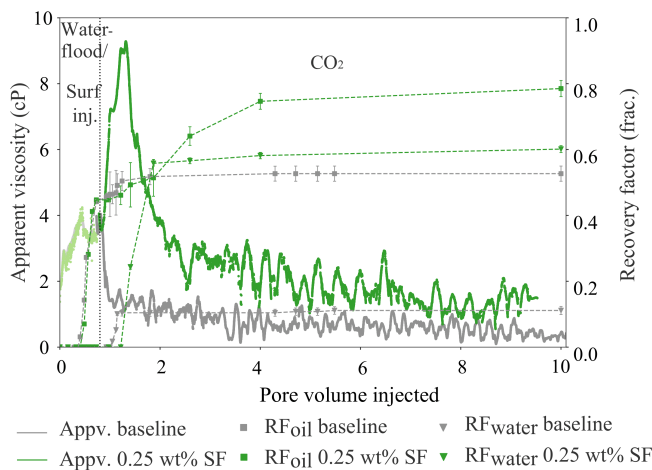


Fig. 5. Apparent viscosity (solid lines) and recovery factors (dotted lines) as a function of pore volume injected for CO₂ injection after waterflood (gray) and after foaming solution injection (green). Results show an increase in apparent viscosity when surfactant was present in the core. Oil and water recovery factors are higher because of foam generation.

compared to 11% for the baseline CO₂ injection. High water recovery is beneficial for CO₂ storage as more pore space can be available to store CO₂.

4.2.3 WAG after waterflood

WAG is a common method to reduce CO₂ mobility and was evaluated to establish a baseline for comparison to SAG experiments for CO₂ EOR and CO₂ storage. Fig. 6 shows an increase in apparent viscosity during WAG compared to the baseline CO₂ injection due to a reduction in CO₂ relative permeability in the presence of higher water saturations (Enick et al., 2012). The apparent viscosity varied between 1 and 3.5 cP during the WAG cycles and rapidly decreased to the same

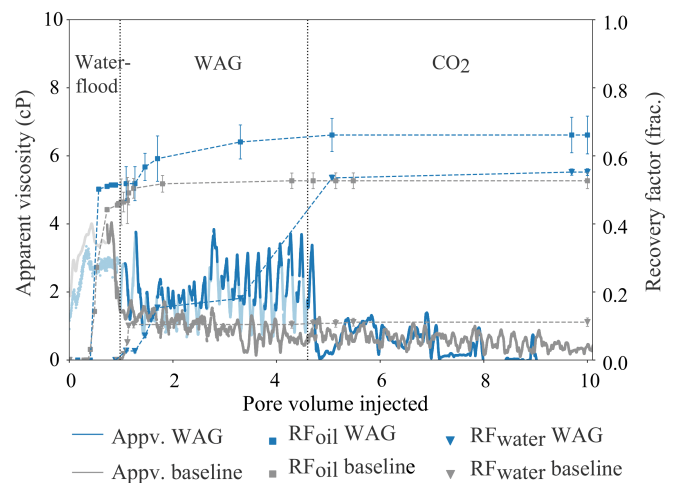


Fig. 6. Apparent viscosity (solid lines) and recovery factors (dotted lines) as a function of pore volume injected for WAG (blue) and baseline CO₂ injection (gray) for comparison. Light and dark colors represent brine and CO₂ injection respectively. Apparent viscosity increased due to CO₂ relative permeability reduction. Oil and water recovery factors are higher than for baseline.

values as the baseline when only CO₂ was injected. This was due to the decrease in water saturation and increase in CO₂ relative permeability. As a result of mobility control through WAG, 15% of additional oil was displaced compared to 8% during the baseline CO₂ injection. Water recovery factor showed improved water displacement for WAG (55%) compared to CO₂ baseline (11%) which increased the CO₂ storage capacity.

4.2.4 SAG after waterflood

Two SAG injections with different surfactant concentrations were performed to evaluate the effect of surfactant concentration of foam strength, stability and CO₂ EOR and CO₂ storage potential. Fig. 7 shows apparent viscosity, oil recovery factor and water recovery factor for 0.25 wt% (green) and 0.50 wt% (red) foaming solution and WAG (blue). An increase in apparent viscosity was observed when surfactant was present in the solution, indicating foam generation. For both solutions the apparent viscosity started to increase after the second SAG cycle. Within each cycle the apparent viscosity increased for the CO₂ slugs and decreased for the surfactant slugs which indicated foam generation in a drainage-like process as also observed by (Kovscek and Radke, 1994). For the 0.25 wt% foaming solution, the apparent viscosity stabilized after 6 cycles and was on average 7 cP. After 18 SAG cycles, pure CO₂ was injected which resulted in a rapid decrease in apparent viscosity. This can be explained by the dry out effect. When pure CO₂ was injected into the core, the foaming solution saturation decreased, gas fraction increased and coarsening of foam occurred. The rate of foam generation and coalescence equated and foam started to collapse or dry out (Abbaszadeh et al., 2014). The apparent viscosity remained higher for the SAG, compared to the WAG, for several PVs CO₂ injected. This indicated trapped gas bubbles within the pores that con-

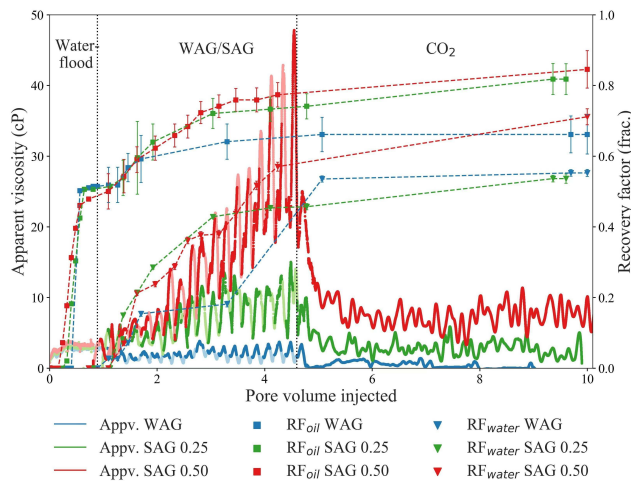


Fig. 7. Apparent viscosity (solid lines) and recovery factors (dotted lines) as a function of pore volume injected for WAG (blue), SAG with 0.25 wt% foaming solution (green) and SAG with 0.50 wt% foaming solution (red). Light and dark colors represent brine and CO₂ injection respectively. CO₂ foam was generated in presence of surfactant indicated by increase in apparent viscosity. Foam increased oil and water recovery.

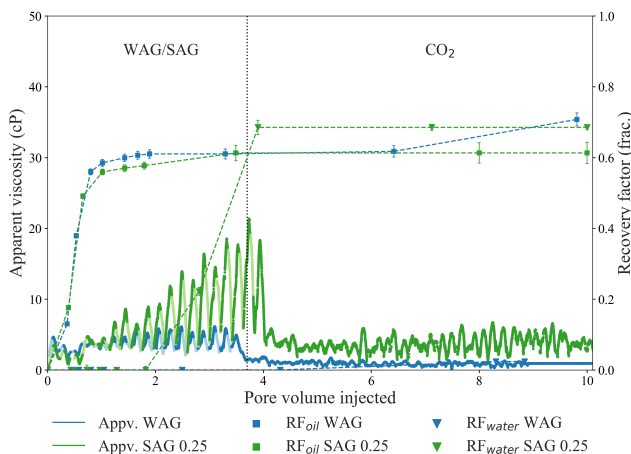


Fig. 8. Apparent viscosity (solid lines) and recovery factors (dotted lines) as a function of pore volume injected for WAG (blue) and SAG (green) as primary recovery method. Light and dark colors represent brine and CO₂ injection respectively. During SAG foam was generated after a significant amount of oil was displaced. Water recovery was higher during SAG compared to WAG.

tributed to continued CO₂ mobility reduction (Jones et al., 2018; Benali et al., 2022).

For the 0.50 wt% foaming solution the apparent viscosity continued to increase even after 18 SAG cycles indicating generation of stronger foam as the injection continued. A rapid decrease in apparent viscosity was observed when pure CO₂ was injected. The apparent viscosity remained one order of magnitude higher than during WAG for several PVs injected indicating CO₂ mobility reduction. Comparison of the two foaming solutions showed stronger foam generation using the

higher surfactant concentration and increased CO₂ mobility reduction.

Generation of CO₂ foam during SAG increased oil and water displacement compared to WAG where no foam was generated. Before WAG and SAG cycles waterflood was performed and approximately 50% of OOIP was recovered for the three experiments. During WAG a total of 66% of OOIP was recovered and the oil recovery stopped after ended WAG cycles. During the SAG injections the total oil recovery was 82%-85% of which 9% OOIP was produced during the pure CO₂ injection stage. Higher apparent viscosity using 0.50 wt% foaming solution did not show significant improvement in oil recovery. This has been observed earlier and is economically beneficial for designing foam formulations for use at the field-scale (Alcorn et al., 2019). An increase in water recovery was also observed when foam was generated. More than 50% of the water was displaced during WAG and 0.25 wt% SAG and 70% was displaced during 0.50 wt% SAG. The increase in foam apparent viscosity had a significant effect on water displacement which resulted in more pore space available for CO₂ storage (Føyen et al., 2020).

4.2.5 WAG and SAG after drainage

WAG and SAG injection methods were implemented directly after primary drainage (i.e., no initial waterflood) with an initial oil saturation of approximately 70%. Fig. 8 shows the apparent viscosity, oil recovery and water recovery for WAG (blue) and SAG (green) as a function of PV injected. During the first 5 cycles, the apparent viscosity and oil recovery was similar for the two injection strategies. After 1.5 PVs injected the apparent viscosity started to increase indicating foam generation. At that point approximately 60% of the OOIP was recovered and oil saturation in the core was 30%. The delay in foam generation compared to SAG after waterflood (Fig. 7, green solid curve) was influenced by the presence of oil. The high amount of mobile oil in the core limited foam generation until the oil saturation was below a critical oil saturation for foam to generate (Friedmann and Jensen, 1986; Mannhardt et al., 1998). Higher apparent viscosity was observed compared to SAG after waterflood (Fig. 7, green curve), which is due to generation of oil/water emulsions in addition to CO₂ foam (Amirmoshiri et al., 2018; Alcorn et al., 2020). Similar to foam, emulsions can contribute to increased flow resistance, hence increased apparent viscosity (McAuliffe, 1973). The apparent viscosity for WAG after drainage was also higher than for WAG after waterflood (Fig. 7, blue solid curve) because of higher flow resistance at higher oil saturations. Foam and emulsions did not contribute to increase the oil recovery as the most part of oil was recovered before foam generation started. However, an improvement in water displacement was observed. During the SAG, 70% of the water was displaced whereas only 3% of water was displaced during WAG. After the 18 WAG and SAG cycles, pure CO₂ was injected into the core for additional 6 to 7 PVs. The apparent viscosity for WAG rapidly decreased to the same values as baseline CO₂ injection because of foam dry out (Fig. 6, gray solid curve). For the SAG, the apparent viscosity remained higher than baseline CO₂ injection due to trapped CO₂ bubbles in the pore

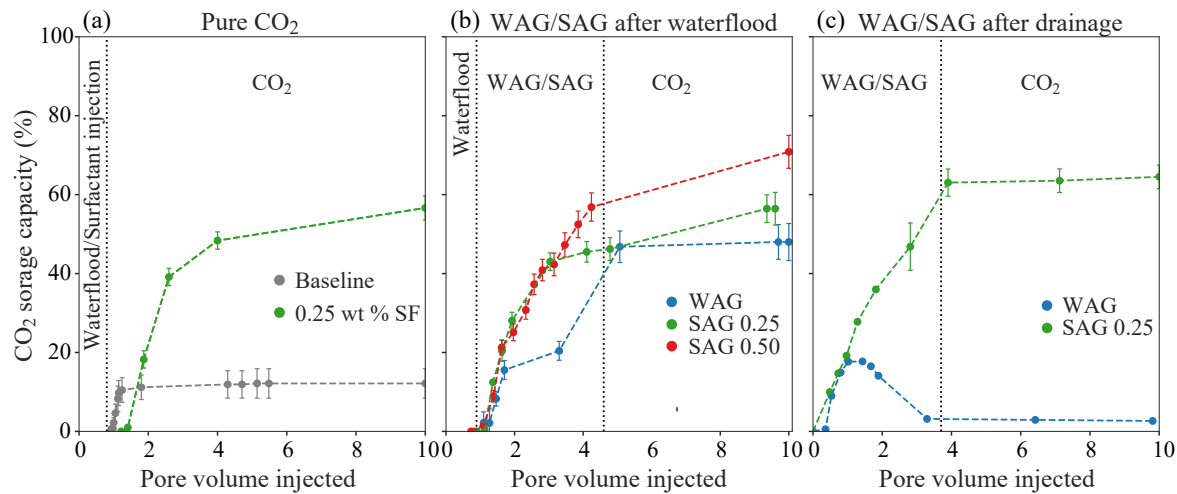


Fig. 9. CO₂ storage capacity versus pore volume injected for the different injection strategies. (a) Pure CO₂ injection after waterflood (gray) and after surfactant injection (green), (b) WAG (blue), SAG with 0.25 wt% (green) and SAG with 0.50 wt% (red) surfactant concentration performed after waterflood, (c) WAG (blue) and SAG (green) performed after drainage. CO₂ foam increased CO₂ storage capacity for all injection strategies.

space, which continued to reduce the CO₂ mobility. Overall, the results did not show improvement in oil displacement when using WAG and SAG directly after drainage compared to WAG and SAG implemented after waterflood.

4.2.6 CO₂ storage

Fig. 9 shows CO₂ storage capacity versus pore volume injected for the different injection strategies. For the baseline CO₂ injection (Fig. 9(a), gray), the storage potential was 12% which was the lowest compared to the other injections. This was because of poor water and oil displacement. Changing the injection strategy to WAG increased storage potential to approximately 50% (Fig. 9(b), blue). Higher storage potential was estimated for all experiments containing foaming solution due to foam generation and improved fluid displacement. The injections containing 0.25 wt% foaming solution resulted in a CO₂ storage capacity of approximately 55% to 60% (Fig. 9(a), Fig. 9(b), Fig. 9(c), green). The highest CO₂ storage capacity (70%) was when stronger foam was generated using 0.50 wt% foaming solution (Fig. 9(b), red). Comparison of WAG after waterflood (Fig. 9(b), blue) and WAG after drainage (Fig. 9(c), blue) showed higher CO₂ storage capacity for WAG after waterflood. The CO₂ storage capacity for WAG after drainage was low because of poor water displacement. Comparison of SAG after waterflood (Fig. 9(b), green) and SAG after drainage (Fig. 9(c), green) showed higher CO₂ storage capacity for SAG after drainage. This was likely due to generation of oil/water emulsions in addition to CO₂ foam which contribute to increased displacement. Overall, foam generation reduced CO₂ mobility, increased displacement and therefore improved the storage capacity.

5. Conclusions

Understanding unsteady-state in-situ CO₂ foam behavior is important for upscaling and implementation of CO₂ foam

for EOR and associated CO₂ storage at the field-scale. The primary objective was to reduce CO₂ mobility, through the generation of foam, in experiments that are representative of field-scale injection strategies. A secondary objective was to investigate the effect of oil on CO₂ foam generation and stability. Therefore, this work focused on establishing a knowledge base and procedure for investigating core-scale unsteady-state CO₂ foam injection strategies. Pure unsteady-state CO₂ injection, WAG and SAG were performed at reservoir conditions and evaluated based on apparent viscosity, oil and water recovery and CO₂ storage capacity. The following key observations and conclusions were drawn:

- Foam quality scans showed that the optimal gas fraction (highest apparent viscosity) was between 0.50 and 0.60 for both surfactant concentrations (0.25 wt% and 0.50 wt%). Rate scans showed a near-Newtonian foam behavior where foam strength was independent of the superficial velocity.
- Injecting foaming solution before CO₂ injection generated foam and improved oil and water displacement compared to only waterflooding before CO₂ injection.
- Reduction of CO₂ relative permeability during WAG increased oil and water recovery compared to the CO₂ baseline, where only CO₂ was injected.
- Generation of CO₂ foam during SAG improved oil displacement by 25% and 50% compared to WAG and to the CO₂ baseline, respectively.
- Foam increased CO₂ storage capacity by 20% to 40% compared to WAG and 350% to 450% compared to the CO₂ baseline.
- Increasing surfactant concentration from 0.25 wt% to 0.50 wt% increased foam apparent viscosity and resulted in improved water displacement and increased CO₂ storage capacity but did not have an impact on oil recovery.
- High oil saturations during WAG and SAG injections

directly after drainage hindered CO₂ foam generation until a critical oil saturation of 30% was reached. In addition to CO₂ foam, generation of oil/water emulsions was observed. Performing WAG and SAG directly after drainage did not have impact on oil recovery compared to WAG and SAG after waterflood.

Acknowledgement

The authors wish to acknowledge the Research Council of Norway PETROMAKS2 program for financial support under grant number 301201 - Optimizing CO₂ Foam EOR Mobility Control for Field Pilots.

Conflict of interest

The authors declare no competing interest.

Open Access This article is distributed under the terms and conditions of the Creative Commons Attribution (CC BY-NC-ND) license, which permits unrestricted use, distribution, and reproduction in any medium, provided the original work is properly cited.

References

- Abbaszadeh, M., Nia Korrani, A. K., Lopez-Salinas, J. L., et al. Experimentally-based empirical foam modeling. Paper SPE 169888 Presented at SPE Improved Oil Recovery Symposium, Tulsa, Oklahoma, USA, 12-16 April, 2014.
- Alcorn, Z. P., Føyen, T., Gauteplass, J., et al. Pore- and core-scale insights of nanoparticle-stabilized foam for CO₂-enhanced oil recovery. *Nanomaterials*, 2020, 10(10): 1917.
- Alcorn, Z. P., Føyen, T., Zhang, L., et al. CO₂ foam field pilot design and initial results. Paper SPE 200450 Presented at SPE Improved Oil Recovery Conference, Virtual, 31 August-4 September, 2020.
- Alcorn, Z. P., Fredriksen, S. B., Sharma, M., et al. An integrated carbon-dioxide-foam enhanced-oil-recovery pilot program with combined carbon capture, utilization, and storage in an onshore Texas heterogeneous carbonate field. *SPE Reservoir Evaluation & Engineering*, 2019, 22(4): 1449-1466.
- Alvarez, J. M., Rivas, H. J., Rossen, W. R. Unified model for steady-state foam behavior at high and low foam qualities. *SPE Journal*, 2001, 6(3): 325-333.
- Amirmoshiri, M., Zeng, Y., Chen, Z., et al. Probing the effect of oil type and saturation on foam flow in porous media: Core-flooding and nuclear magnetic resonance (NMR) imaging. *Energy & Fuels*, 2018, 32(11): 11177-11189.
- Benali, B., Føyen, T. L., Alcorn, Z. P., et al. Pore-scale bubble population dynamics of CO₂-foam at reservoir pressure. *International Journal of Greenhouse Gas Control*, 2022, 114: 103607.
- Bjørlykke, K. *Petroleum Geoscience: From Sedimentary Environments to Rock Physics*. Heidelberg, German, Springer, 2010.
- Chang, S.-H., Grigg, R. B. Effects of foam quality and flow rate on CO₂-foam behavior at reservoir temperature and pressure. *SPE Reservoir Evaluation & Engineering*, 1999, 2(3): 248-254.
- Chang, S. H., Owusu, L. A., French, S. B., et al. The effect of microscopic heterogeneity on CO₂-foam mobility: Part 2-mechanistic foam simulation. Paper SPE 20191 Presented at SPE/DOE Enhanced Oil Recovery Symposium, Tulsa, Oklahoma, 22-25 April, 1990.
- Chou, S. I., Vasicek, S. L., Pisio, D. L., et al. CO₂ foam field trial at north ward-estes. Paper SPE 24643 Presented at 67th Annual Technical Conference and Exhibition of the Society of Petroleum Engineers, Washington, D. C., 4-7 October, 1992.
- Christensen, J. R., Stenby, E. H., Skauge, A. Review of wagg field experience. *SPE Reservoir Evaluation & Engineering*, 2001, 4(2): 97-106.
- Enick, R. M., Olsen, D. K., Ammer, J., et al. Mobility and conformance control for carbon dioxide enhanced oil recovery (CO₂-EOR) via thickeners, foams, and gels—A detailed literature review of 40 years of research. Paper SPE 154122 Presented at SPE Improved Oil Recovery Symposium, Tulsa, Oklahoma, 14-18 April, 2012.
- Falls, A. H., Musters, J. J., Ratulowski, J. The apparent viscosity of foams in homogeneous bead packs. *SPE Reservoir Engineering*, 1989, 4(2): 155-164.
- Farajzadeh, R., Andrianov, A., Krastev, R., et al. Foam-oil interaction in porous media: Implications for foam assisted enhanced oil recovery. *Advances in Colloid and Interface Science*, 2012, 183-184: 1-13.
- Farajzadeh, R., Lotfollahi, M., Eftekhari, A. A., et al. Effect of permeability on implicit-texture foam model parameters and the limiting capillary pressure. *Energy & Fuels*, 2015, 29(5): 3011-3018.
- Føyen, T., Brattekkås, B., Fernø, M. A., et al. Increased CO₂ storage capacity using CO₂-foam. *International Journal of Greenhouse Gas Control*, 2020, 96: 103016.
- Friedmann, F., Jensen, J. A. Some parameters influencing the formation and propagation of foams in porous media. Paper SPE 15087 Presented at SPE California Regional Meeting, Oakland, California, 2-4 April, 1986.
- Hoefner, M. L., Evans, E. M. CO₂ foam: Results from four developmental field trials. *SPE Reservoir Engineering*, 1995, 10(4): 273-281.
- Hanssen, J. E., Holt, T., & Surguchev, L. M. Foam processes: An assessment of their potential in north sea reservoirs based on a critical evaluation of current field experience. Paper SPE 27768 Paper presented at the SPE/DOE Improved Oil Recovery Symposium, Tulsa, Oklahoma, 17-20 April, 1994.
- Jones, S. A., Getrouw, N., Vincent-Bonnieu, S. Foam flow in a model porous medium: II. The effect of trapped gas. *Soft Matter*, 2018, 14(18): 3497-3503.
- Jones, S. A., Laskaris, G., Vincent-Bonnieu, S., et al. Surfactant effect on foam: From core flood experiments to implicit-texture foam-model parameters. *Journal of Industrial and Engineering Chemistry*, 2016, 37: 268-276.
- Khatib, Z. I., Hirasaki, G. J., Falls, A. H. Effects of capillary pressure on coalescence and phase mobilities in foams flowing through porous media. *SPE Reservoir Engineering*, 1988, 3(3): 919-926.
- Kovscek, A. R., Radke, C. J. *Fundamentals of foam transport*

- in porous media, in *Foams: Fundamentals and Applications in the Petroleum Industry*, edited by L. L. Schramm, American Chemical Society, Washington, pp. 115-163, 1994.
- Lake, L. W., Johns, R. T., Rossen, W. R., et al. *Fundamentals of enhanced oil recovery*. Richardson, TX: Society of Petroleum Engineers, 2014.
- Lee, H. O., Heller, J. P. Laboratory measurements of CO₂-foam mobility. *SPE Reservoir Engineering*, 1990, 5(2): 193-197.
- Lee, S., Kam, S. I. Chapter 2-Enhanced oil recovery by using CO₂ foams: Fundamentals and field applications, in *Enhanced Oil Recovery Field Case Studies*, edited by J. J. Sheng, Gulf Professional Publishing, Boston, pp. 23-61, 2013.
- Mannhardt, K., Novosad, J. J., Schramm, L. L. Foam/oil interactions at reservoir conditions. Paper SPE 39681 Presented at SPE/DOE Improved Oil Recovery Symposium, Tulsa, Oklahoma, 19-22 April, 1998.
- [Massarweh, O., Abushaikh, A. S. A review of recent developments in CO₂ mobility control in enhanced oil recovery. *Petroleum*, 2021.](#)
- McAuliffe, C. D. Oil-in-water emulsions and their flow properties in porous media. *Journal of Petroleum Technology*, 1973, 25(6): 727-733.
- Metz, B., Davidson, O., De Coninck, H. C., et al. *IPCC Special Report on Carbon Dioxide Capture and Storage*. London, United States, Cambridge University Press for the Intergovernmental Panel on Climate Change, 2005.
- Muller, T., Lake, L. W. Theoretical study of water blocking in miscible flooding. *SPE Reservoir Engineering*, 1991, 6(4): 445-451.
- Osei-Bonsu, K., Grassia, P., Shokri, N. Effects of pore geometry on flowing foam dynamics in 3D-printed porous media. *Transport in Porous Media*, 2018, 124(3): 903-917.
- Osterloh, W. T., Jante, M. J., Jr. Effects of gas and liquid velocity on steady-state foam flow at high temperature. Paper SPE 24179 Presented at SPE/DOE Enhanced Oil Recovery Symposium, Tulsa, Oklahoma, 22-24 April, 1992.
- Peksa, A. E., Wolf, K.-H. A. A., Zitha, P. L. J. Bentheimer sandstone revisited for experimental purposes. *Marine and Petroleum Geology*, 2015, 67: 701-719.
- Pini, R., Krevor, S., Krause, M., et al. Capillary heterogeneity in sandstone rocks during CO₂/water core-flooding experiments. *Energy Procedia*, 2013, 37: 5473-5479.
- Rognmo, A. U., Horjen, H., Fernø, M. A. Nanotechnology for improved CO₂ utilization in ccs: Laboratory study of CO₂-foam flow and silica nanoparticle retention in porous media. *International Journal of Greenhouse Gas Control*, 2017, 64: 113-118.
- Ross, S., McBain, J. W. Inhibition of foaming in solvents containing known foamers. *Industrial & Engineering Chemistry*, 1944, 36(6): 570-573.
- Rossen, W. R. Foams in enhanced oil recovery, in *Foams: Theory, Measurements and Applications*, edited by R. K. Prud'homme and S. A. Khan, Routledge, New York, pp. 413-464, 1996.
- Schramm, L. L. *Foams: Fundamentals and Applications in the Petroleum Industry*. Washington, D. C., American Chemical Society, 1994.
- Shan, D., Rossen, W. R. Optimal injection strategies for foam ior. *SPE Journal*, 2004, 9(2): 132-150.
- Sharma, M. CO₂ mobility control with foam for enhanced oil recovery and associated storage multi-scale approach for field application. Norway, University of Stavanger, 2019.
- Shelton, J. L., Schneider, F. N. The effects of water injection on miscible flooding methods using hydrocarbons and carbon dioxide. *Society of Petroleum Engineers Journal*, 1975, 15(3): 217-226.
- Skauge, A., Aarra, M. G., Surguchev, L., et al. Foam-assisted wag: Experience from the snorre field. Paper SPE 75157 presented at the SPE/DOE Improved Oil Recovery Symposium, Tulsa, Oklahoma, 13-17 April, 2002.
- Song, Y.-C., Zhu, N.-J., Liu, L., et al. Magnetic resonance imaging study on the miscibility of a CO₂/n-decane system. *Chinese Physics Letters*, 2011, 28(9): 096401.
- Tadros, T. F. *Basic Principles of Dispersions*. Berlin/Boston, Germany, De Gruyter, 2017.
- Talebian, S. H., Masoudi, R., Tan, I. M., et al. Foam assisted CO₂-EOR: A review of concept, challenges, and future prospects. *Journal of Petroleum Science and Engineering*, 2014, 120: 202-215.